Journal of Cybernetics and Informatics

published by

Slovak Society for
Cybernetics and Informatics

Volume 13, 2012

http://www.sski.sk/casopis/index.php (home page)

ISSN: 1336-4774

PERFORMANCE OF PARALLEL HYBRID ELECTRIC VEHICLE ELECTRICAL PROPULSION SYSTEM USING DIFFERENT INVERTER CONTROL TECHNOLOGIES

Maged N. F. Nashed[1], Said Wahsh[1], Hamed. G. Hamed[2], and Tarak Dakrory[2]

[1]Electronic Research Institute, Giza, Egypt, phone: 202-33310552, email: maged@eri.sci.eg, wahsh@eri.sci.eg

[2]Faculty of Engineering (at Shubra), Benha University, Egypt

Abstract

This paper present application of electrical propulsion system of the Parallel Hybrid Electric Vehicle (PHEV) using three different Pulse width modulation (PWM) techniques and their results compared in terms of THD, DC voltage utilization, transient behavior, and the required execution time applied. The intelligent Fuzzy Logic Control (FLC) is applied to improve the dynamic performance of PHEV. The electrical motor drive is controlled via PWM-voltage source inverter (VSI), using scalar control method and three types of PWM Sinusoidal PWM (SPWM), conventional Space Vector PWM (SVPWM) and carrier-base SVPWM are analyzed. In the other hand the PHEV system modeled and simulated for different roads (straight, clamping, and down inclination roads).Not only that but also under different road cycle's small federal urban drive (SFUD), and high way (HY). The control algorithm is based on the road cycle and in all it the vehicle is driven at starting with the IM, and the internal combustion engine (ICE) is used mainly in HY road cycle, while the IM is used mainly in the urban-areas to reduce the emissions in it. The hybrid operation is also considered in some parts of the road cycles. The SIMPLEV software program is used to study the vehicle emissions in the different road cycles to ensure that the used control algorithm decreases the vehicle emission in urban areas.

Keywords: Hybrid Electric Vehicles- Induction Motor, Internal Combustion Engine, and Fuzzy Logic Control

1 INTRODUCTION

The transportation system is very important to the entire world today; however, the large number of automobiles, which used around the world, has caused and continues to cause serious problems for the environment and human life. Air pollution, global warming, and the rapid depletion of the Earth's petroleum resources are now problems of paramount concern. In recent decades, the research and development activities related to the transportation have emphasized the development of high efficiency, clean, and safe transportation.

In recent years, activity in alternative fuel research, such as bio-diesel, ethanol, hydrogen, natural gas, and propane has increased rapidly. Also, several of the largest automotive companies (General Motors, Ford, Honda, Nissan, Toyota, etc.) begun to do research on advanced vehicle development. Academic research institutions all over the world have investigate the systems including electric vehicles (EVs), hybrid electric vehicles (HEVs) and fuel cell electric vehicles (FCEVs).

EV uses an electric motor for traction, and chemical batteries, ultra capacitors, and/or flywheels for their corresponding energy sources. EV has many advantages over the conventional ICE vehicle, such as an absence of emissions, high efficiency, independence from petroleum, quiet and smooth operation. HEV use an electric motor with another power source generally is an ICE. HEV has the advantages of very low emission and good performance.

EVs have some advantages over conventional ICE vehicles, such as high energy efficiency and zero environmental pollution. However, the performance, especially the operating range per battery charge, is much smaller than the ICE vehicles, due to the low energy content of batteries [1] and [2].

The implementing range of EVs can be extended by an additional drive, i.e. ICE. So, the vehicles will be supplied with more than one drive and the vehicle is named HEV [3]. HEV architectures are organized into three classes: parallel, series and series- parallel hybrids (complex) [3]. In PHEV configuration, as shown in Fig.1, the engine is mechanically coupled to the electric drive system, the clutch can disconnect each of them. So, the PHEV can operate in the following modes of operation which are: electric motor, ICE or both.

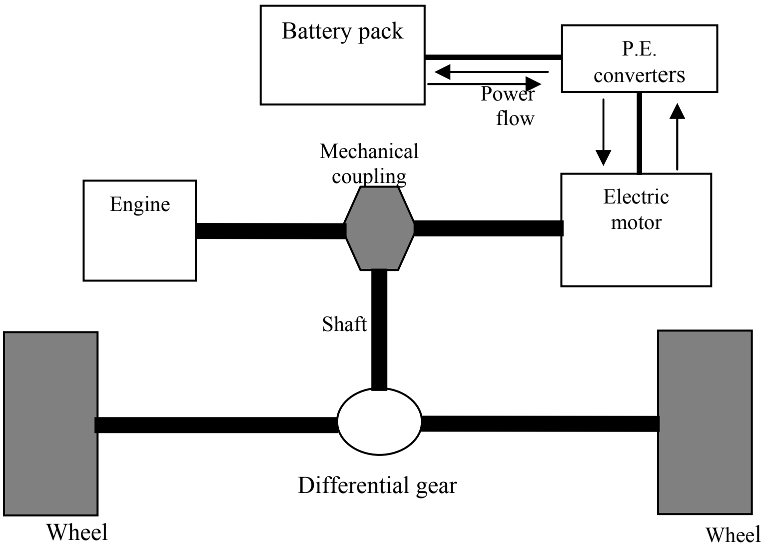

Fig.1. Parallel hybrid electric vehicles.

The main advantages of PHEV are:

1. It needs only two propulsion components (ICE and the motor) because the motor can be used as generator to charge batteries at regenerative braking mode operation.
2. It has smaller ICE and electric motor sizes compared to the series HEV, because power can be summed to meet the required driver power.
3. The low number of power conversions can potentially increase the efficiency of the vehicle, as compared to the series HEV.

The advantages and disadvantages of different types of motors: DC, IM, Permant Magnet Synchronous Motor (PMSM), Switched Reluctance Motor(SRM) and Permant Magnet Brushless DC (BLDC) are listed in Table I, [4] and [5].

Table I. Advantages and disadvantages of different motors types

	Type of motor	Advantages	Disadvantages
1	DC motor	- Known Technology. - Simple control.	- High cost. - Maintenance is required.
2	IM	-Known technology. -Available manufacturing infrastructure.	-Need to extract high rotor loss from the core of the machine. -Needs low pole number requiring large copper end windings and considerable stator back iron.
3	PMSM	High pole number reduces weight and material content. PM excitation rovides high fficiency. -Stator and electronics technology similar to IM.	-Present cost of high energy magnets. -Fixed flux gives low-speed range at constant power. -Magnet corrosion and possible demagnetization.
4	SRM	-Robust and simple construction. -Power semiconductor "shoot-through" failure cannot occur.	-Both stator and electronics are different from established technology. -Intrinsically high torque ripple may cause noise and vibrations. -High peak current and frequency can cause electro magnetic interference problem. - Needs for rotor position sensing.
5	BLDC	-Suitable to be used in high temperature complications. -High power density and efficiency.	-Difficult in use at field weakening. -High cost for permanent magnet. -Needs for rotor position sensing.

2 MODELING OF THE IM DRIVE SYSTEM

The block diagram of IM drive system, which is shown in Fig. 2, contains batteries, PWM-VSI, IM, and mechanical load.

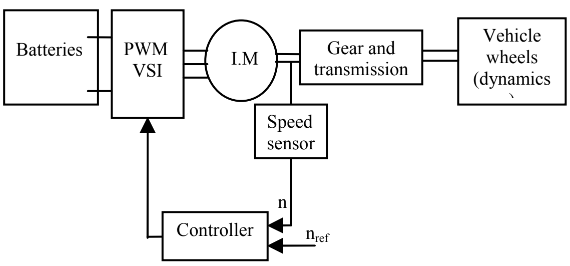

Fig.2. Block diagram of IM drives system.

2.1 Modelling of IM

The equations representing the dynamic modeling of IM are the classical method to describe the dynamic model of it, and get first for the three- phase of both the stator and the rotor, [6]:

$$u_s = r_s i_s + \frac{d\lambda_s}{dt} \tag{1}$$

$$u_r = r_r i_r + \frac{d\lambda_r}{dt} \tag{2}$$

And the rotor is short circuited, the rotor voltage components (uqr and udr) are equal zero, and the rotor current components (idr and iqr) are reversed. So, the equations of IM are [6]:

$$u_{ds} = i_{ds} r_s + L_s \frac{di_{ds}}{dt} - M \frac{di_{dr}}{dt} \tag{3}$$

$$u_{qs} = i_{qs} r_s + L_s \frac{di_{qs}}{dt} - M \frac{di_{qr}}{dt} \tag{4}$$

$$0 = M \frac{di_{ds}}{dt} - M\omega_r i_{qs} - r_r i_{dr} - L_r \frac{di_{dr}}{dt} + L_r \omega_r i_{qr} \tag{5}$$

$$0 = M \frac{di_{qs}}{dt} + M\omega_r i_{ds} - r_r i_{qr} - L_r \frac{di_{qr}}{dt} - L_r \omega_r i_{dr} \tag{6}$$

In order to simulate the above equations, they are arranged as follows:

$$\frac{di_{ds}}{dt} = \frac{1}{L_s L_r - M^2}\left[u_{ds} L_r - i_{ds} L_r r_s - i_{qs} M^2 \omega_r - i_{dr} r_r M + i_{qr} M L_r \omega_r\right] \tag{7}$$

$$\frac{di_{qs}}{dt} = \frac{1}{L_s L_r - M^2}\left[u_{qs} L_r + i_{ds} M^2 \omega_r - i_{qs} L_r r_s - i_{dr} M L_r \omega_r - i_{qr} r_r M\right] \tag{8}$$

$$\frac{di_{dr}}{dt} = \frac{1}{L_s L_r - M^2}\left[u_{ds} M - i_{ds} r_s M - i_{qs} M L_s \omega_r - i_{dr} r_r L_s + i_{qr} L_s L_r \omega_r\right] \tag{9}$$

$$\frac{di_{qr}}{dt} = \frac{1}{L_s L_r - M^2}\left[u_{qs} M + i_{ds} M L_s \omega_r - i_{qs} r_s M - i_{dr} L_s L_r \omega_r - i_{qr} r_r L_s\right] \tag{10}$$

Then motor electro-mechanical equation as follows:

$$J \frac{d\omega_m}{dt} = T_e - T_L - B\omega_m \tag{11}$$

Where

$$T_e = M[i_{qs}\, i_{dr} - i_{qr}\, i_{ds}] \tag{12}$$

2.2 Modelling of different PWM VSI techniques

There are three PWM techniques used, to control the VSI are as follows:

1- The SPWM technique is based on the comparison between the three sinusoidal symmetric voltage waveforms (control signals), which have a frequency equal to the required fundamental frequency, with a triangular waveform (carrier signal), which has a frequency equal to the switching frequency (Fs).

2- The conventional SVPWM technique which is based on the calculations of different switching time intervals for each voltage sector, the switching period of each switch at any sector depends on the two vectors belonging to this sector:

3- The carrier-based SVPWM technique is based on obtaining the switching periods of each switch by comparing a three control signals (sinusoidal waveforms) with a triangular (carrier) waveform.

The three control signals are injected by a third harmonic waveform. The mathematical equation that describes the control waveforms for the carrier based SVPWM technique is as follows [7]:

$$u_{1c} = U_{\max} \sin(\omega_c t) - [\frac{\max(u_1 + u_2 + u_3)}{2} + \frac{\min(u_1 + u_2 + u_3)}{2}] \quad (13)$$

$$u_{2c} = U_{\max} \sin(\omega_c t - 2 * \pi / 3) - [\frac{\max(u_1 + u_2 + u_3)}{2} + \frac{\min(u_1 + u_2 + u_3)}{2}] \quad (14)$$

$$u_{3c} = U_{\max} \sin(\omega_c t + 2 * \pi / 3) - [\frac{\max(u_1 + u_2 + u_3)}{2} + \frac{\min(u_1 + u_2 + u_3)}{2}] \quad (15)$$

Where: u1c, u2c, and u3c are the instantaneous control voltage components for the carrier-based SVPWM. The intersection points for each control waveform and the triangular waveform determine the switching intervals for each switch in the different sectors.

2.3 Modeling of the ICE

The ICE is a complex assembly contains a variety of components that are designed on the basis of aerodynamic laws. A mathematical model of the engine with individual components is complicated [8]. So, there are different methods to simulate the ICE. In this work the ICE is modeled by two different methods: the first model of the ICE is obtained by using a simple model [9]. The second model is obtained as a look-up table model using the SIMPLEV program.

The first model of the ICE [6] includes a two-state dynamic model, whose output is the ICE torque.

$$\begin{aligned} \dot{x}_1 = & -280.92 - \frac{3337.3}{x_1} + 818.77 x_2 - 307.29 x_2^2 + 0.91185 * x_1 * x_2 \\ & + 0.24428 x_1 - 0.000764 x_1^2 - 7.1429 T_{load} \end{aligned} \quad (16)$$

$$\begin{aligned} \dot{x}_2 = & 0.15126 - 0.0371 * x_1 * x_2 + 0.01393 * x_1 * x_2^2 - 0.00004133 * x_1^2 * x_2 \\ & + 0.41328 * g(x_2) * u \end{aligned} \quad (17)$$

$$\begin{aligned} T_{eng} = & -39.32 - \frac{467.22}{x_1} + 114.62 x_2 - 43.02 * x_2^2 + 0.1276 * x_1 * x_2 \\ & + 0.03419 * x_1 - 0.000107 * x_1^2 \end{aligned} \quad (18)$$

$$\begin{aligned} & g(p_m) = 1 && if \ \frac{p_m}{p_{amb}} \le 0.5 \\ & g(p_m) = \frac{2}{p_{amb}} \sqrt{p_{amb} * p_m - p_m^2} && if \ \frac{p_m}{p_{amb}} \rangle 0.5 \end{aligned} \quad (19)$$

$$u = 2.821 - 0.05231 \theta_e + 0.10299 \theta_e^2 - 0.00063 \theta_e^3 \quad (20)$$

2.4 Modeling of the controllers

The two types of controllers, which are used in this work, are the classical (conventional) PI controller and the FLC as intelligent controller. The values of membership functions are in per unit (p.u) and there are gain values in the simulation model for input and output values. There are two fuzzy variables and seven linguistic variables. The designed rules give good results nearly to the model control surface to reach the aim of the control strategy.

3 SIMULATION OF THE ELECTRICAL PROPULSION SYSTEM

The previous analysis is conducted using a constant mechanical load. In this section the analysis is conducted using vehicle torque as the mechanical load torque for the IM drive system as shown in Fig. 2.

3.1 Simulation of the System Using SPWM

The simulation block diagram of IM drive system using the SPWM technique is in Fig. 3.

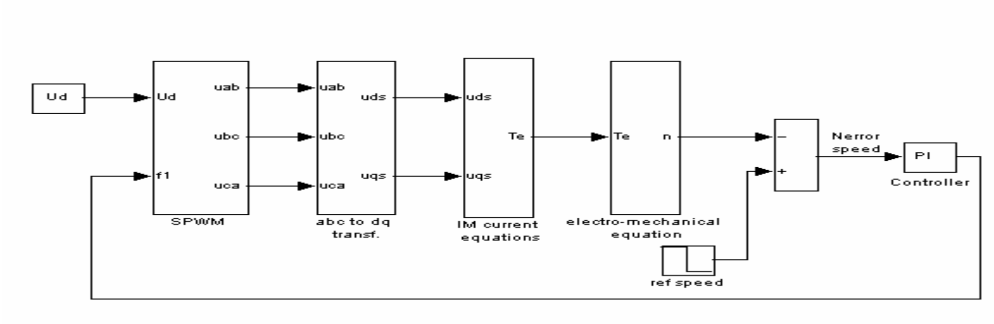

Fig. 3. Simulation block diagram of IM drive system.

The sequence of the system analysis is as follows:

1. According to the required speed, the speed controller adjusts the suitable required fundamental frequency (f1).
2. The frequency of the control voltage waveforms (vcontrol(a) , vcontrol(b) , and vcontrol(c)) of the SPWM is the fundamental frequency from the controller, so the three phase output voltage from the SPWM has the same fundamental frequency.
3. The magnitude of the motor line voltages are controlled by the modulation index which depends on the ratio of the (V/f) is kept constant.
4. Using the park transformation the three phase voltages (uab, ubc, and uca) are transformed to two-phase components (d-q) with the same frequency.
5. The voltage components (uds, udq) are applied to the IM subsystem and the motor output speed signal is compared with the reference speed and the error speed (Nerror) is entered to the controller. The simulation result of the speed response using PI control is shown in Fig. 4

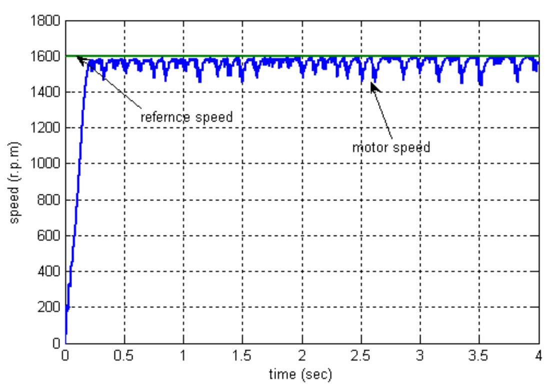

Fig.4. Speed response using PI controller.

3.2 Simulation using the FLC

The simulation result of the speed response using the FLC is shown in Fig. 5.

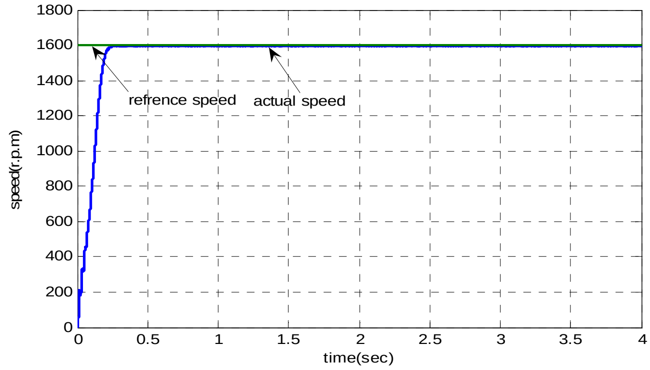

Fig.5. Speed response of IM using FLC.

3.3 Comparison between performance characteristics of the system using SPWM

The system performance is obtained with different operating conditions using a speed disturbance, a torque disturbance, and changing of the SPWM control parameters (modulation index and frequency modulation index), [10]. The first case is the simulation of the system under the parameters (reference speed =1500 r.p.m, load torque = 10 Nm, ma = 0.95, and mf = 13). And second case when ma is changed from 0.95 to 0.75. While third case for state ma=0.95 and mf = 65. The results of three cases are shown in Fig. 6. And the compare of results are in table 2.

First case m_a=0.95, m_f = 13. Second case m_a=0.75, m_f = 13. Third case m_a=0.95, m_f = 65

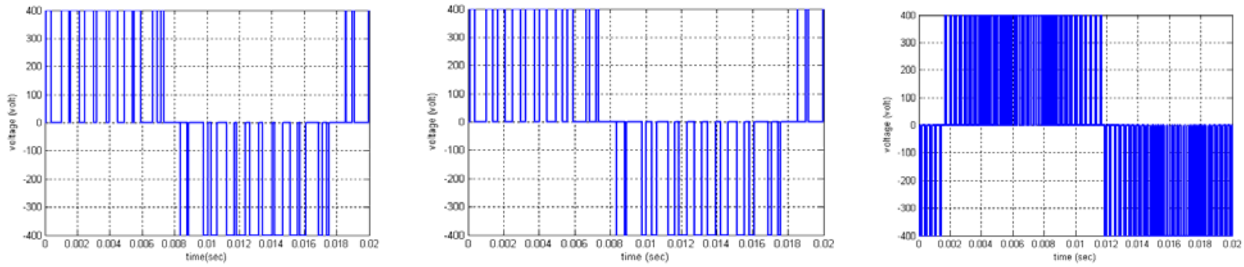

Motor line voltage

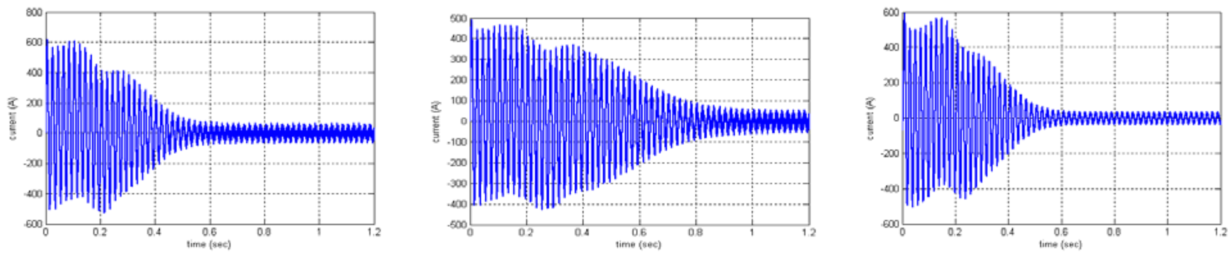

Motor line current.

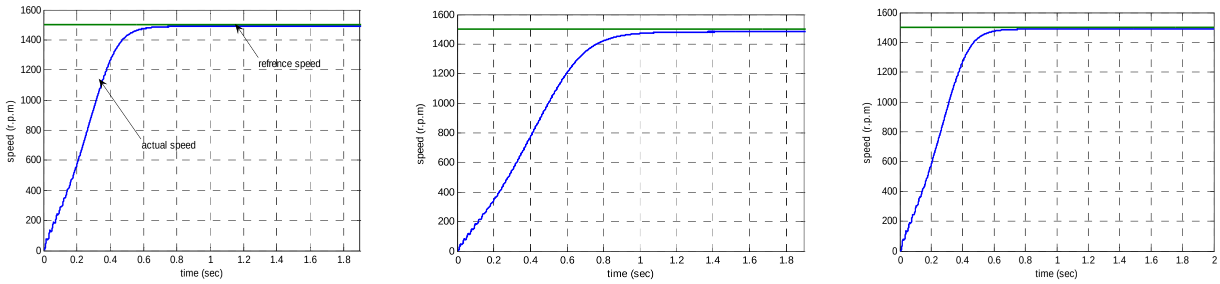

Motor speed

Fig. 6. The results of three case of SPWM.

Table II. Comparison between results of SPWM.

	m_a=0.95, m_f = 13.	m_a=0.75, m_f = 13.	m_a=0.95, m_f = 65
S. S. Time sec	**0.8**	**1.45**	**0.72**
Max. start current Amp.	**600**	**450**	**550**
Harmonic current %	**0.72**	**0.72**	**0.59**

3.4 Performance characteristics of the system using conventional SVPWM)

The conventional SVPWM technique is also applied to the IM drive system to study the performance of the system in this case.

3.5 Performance characteristics of the system using carrier based SVPWM

The carrier-based SVPWM technique is also applied to the IM drive system to study the performance of the system in this case. The performance of the system is studied for three cases using SPWM, conventional SVPWM and carrier-based SVPWM, [11].

The first results of the system for all control are shown in Fig. 7, when change the load torque of the motor from 10 Nm to 120 Nm. And other results when the reference speed changes from 1500 rpm to 1000 rpm are shown in Fig. 7.

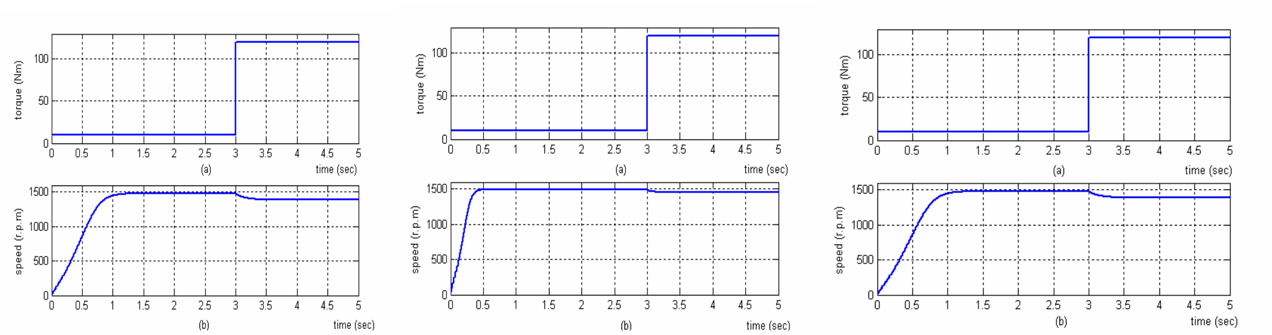

SPWM Conventional SVPWM carrier-based SVPWM

Fig. 7. System performance under varying the load torque

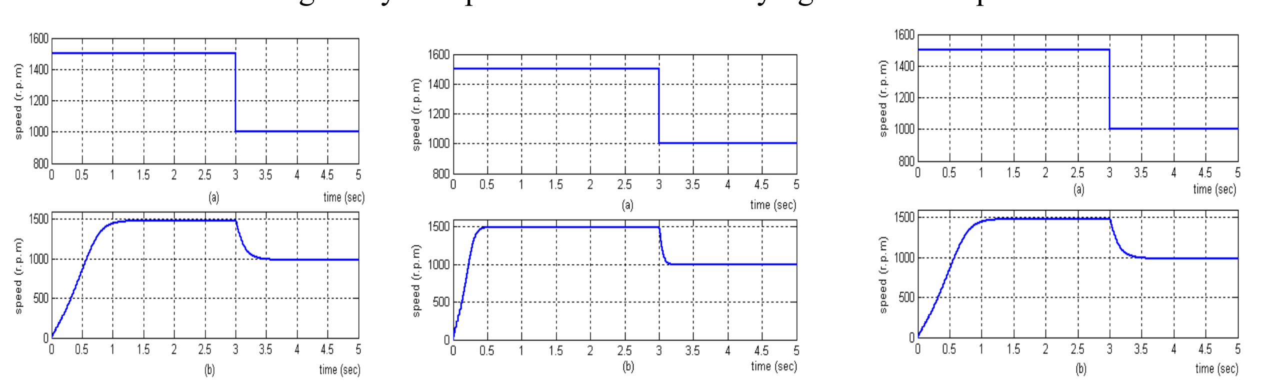

SPWM Conventional SVPWM carrier-based SVPWM

Fig.8. System performance under varying reference speed.

3.6 Performance comparison of the electrical propulsion system using the three PWM techniques

Using different PWM techniques affect mainly the harmonic contents, the DC voltage utilization, and the transient response of the electric propulsion system. A compression has been done among three PWM techniques considering these three aspects. The transient response of the electric propulsion system for the three PWM techniques is shown in Fig. 9 for the motor speed. It is clear from this figure that the conventional SVPWM has the best transient performance. The comparison among the three PWM techniques is shown in Table III.

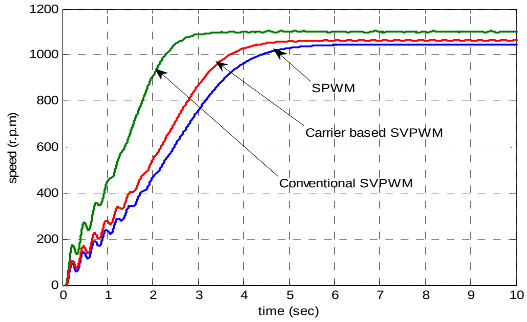

Fig. 9. Motor speed transient response of the three different PWM techniques.

The comparison shows from Table 3 that the conventional SVPWM has the lowest THD, the highest DC voltage utilization, and the lowest transient time required to reach the steady states but it has the largest time to execute the simulation program process because of the complexity of the calculations of the switching time intervals.

On the other side, the carrier based SVPWM is an intermediate choice for the different performance parameters with the lowest computation time for simulation.

Table III. Comparison of the three PWM techniques.

PWM type	THD for line voltage	THD for motor line current	Fundamental voltage as P.U from DC voltage supply	Transient time for vehicle speed (sec.)	Execution time as P.U from simulation time (sec.)
SPWM	7.98%	4.23%	0.74	6	20
Conventional SVPWM	6.23%	3.19%	0.9	4	115
Carrier based SVPWM	6.85%	3.96%	0.79	5	18

4 SIMULATION OF THE PHEV

4.1 FLC of ICE

The model of the ICE shows that the speed of the engine can be controlled by changing the throttle angle (θ) .So, the FLC can be applied to the ICE such that the engine error speed is the input of the FLC and the θ is the output of the FLC according to the reference speed.

The simulation result of the engine speed response using the FLC is shown in Fig. 10. It can be shown that the dynamic response of engine speed using the FLC is better than the case of open loop (without controller).

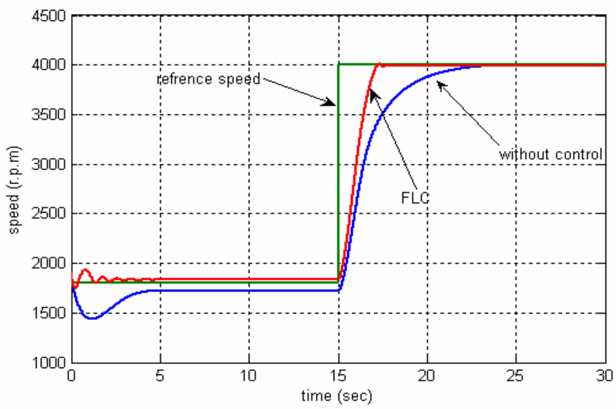

Fig. 10. Engine speed response using the FLC.

4.2 Simulation results of the system with different road cycles

The simulation results were obtained in different road cycles, to study the performance of the PHEV in these cycles. There are two road cycles considered in this study which are: SFUD, and HY.

4.2.1 Simulation results under SFUD cycle

SFUD cycle is consists of a stop and go urban driving profile with a total time of 360 seconds. The simulation results of the PHEV system under SFUD cycle are shown in Fig. 11. The IM is used for driving the vehicle alone in most parts of the SFUD cycle, while the ICE is used as an assistor to the IM for driving the vehicle in some parts of the cycle at which the speed is more than 60 km/hr.

4.2.2 Simulation results under HY cycle

HY cycle, contains up and down speeds in a non-urban area with time of 765 seconds. PHEV system is modeled under HY cycle as shown in Fig. 12.

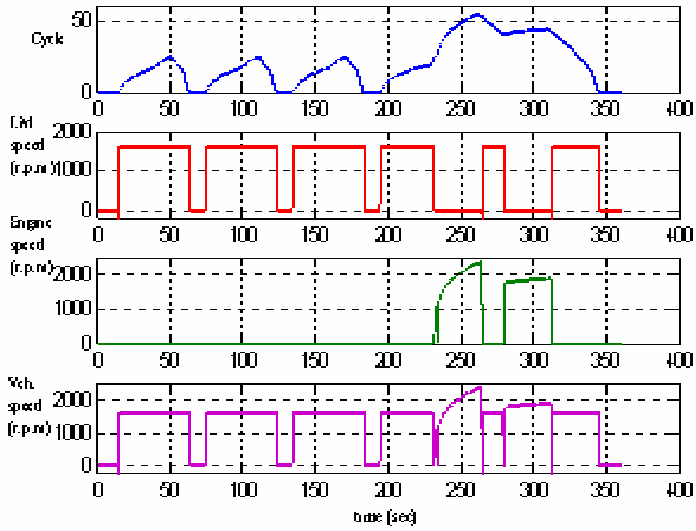

Fig. 11. Various speeds of PHEV with SFUD road cycle.

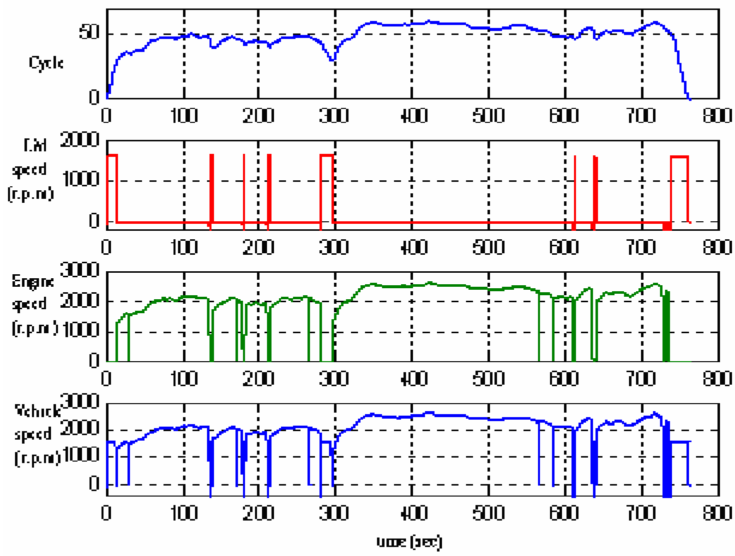

Fig. 12. Various speeds of PHEV with HY

The electrical motor drive is controlled via PWM-VSI, using scalar control method and three types of PWM SPWM, conventional SVPWM, and carrier-base SVPWM are and compared. The results show that the THD using the SVPWM is less than that of using the carrier-base SVPWM. But the advantage of the carrier based SVPWM that it has less execution time and easier in implementation.

5 CONCLUSIONS

In this paper FLC is applied to the heart of the PHEV, electrical motor drive system, and ICE. The simulation results using Matlab/ Simulink software package show that the system performance is stable and has good dynamic response under different operating conditions. Also, the vehicle is simulated under different road cycles, and the results shows that the electrical motor drive is used for starting and at the urban areas but ICE drive used in the high way areas.

Appendix

(1) I.M parameters are:

P_{rated}	37 kW
V_L	460V
f	60Hz
2p	4
n_{rated}	1780 r.p.m
r_s	0.087 Ω
rr	0.228 Ω
L_s	0.00008 H
L_r	0.00008 H
M	0.0347 H
J	1.662 kg. m2
B	0.12 N.m.s

2) ICE parameters

Pe (max)	40 kW
Fuel	20 liters
ne	9000 r.p.m
gr2	3.6

List of symbols

A_0,...A_8 constant equation factors
β friction constant
i_s and i_r stator and rotor phase currents.
J motor inertia constant
M Mutual magnetizing inductance
P_m engine pressure,
P_{amb} ambient pressure.
r_s and r_r i stator and rotor resistance.
T_e developed motor (electromagnetic) torque,
T_{eng} ICE torque
T_{load} load torque
u_s and u_r stator and rotor phase voltages.
u variable function of the throttle angle
ω_m mechanical angular speed of the motor.
ω_r Rotor angular velocity
x_1 states of the ICE model are the speed
x_2 manifold pressure
θ_e throttle angle
λ_s and λ_r stator and rotor flux linkages.

REFERENCES

[1] S. Imai, Nobuaki and Y. Horii: Total Efficiency of a Hybrid Electric Vehicle. IEEE, PCC-Nagaoka, 1997, pp. 947-950.
[2] J. Larminie and J. Lowry: Electric Vehicle Technology Explained. Book, John Wiley & Sons Ltd, Copyright 2003.
[3] H. Ucarol, A. Kaypmaz and R. T. Okan: A Performance Comparison Study among Conventional, Series Hybrid and Parallel Hybrid Vehicles. www.emo.org.tr/ekler/c792a8279211dec ek.pdf.
[4] M. Eshani, K. M.Rahman and H. A.Toliyat: Propulsion System Design of Electric and Hybrid Vehicles. IEEE Transactions on Industrial Electronics, Vol. 44, No.1, Feb. 1997, pp. 19-27.

[5] C. C. Chan: An Overview of Power Electronics in Electric Vehicles. IEEE Transactions on Industrial Electronics, Vol. 44, No.1, Feb. 1997, pp. 3-13.
[6] R. Toufouti, S. Meziane, and H. Benalla: Direct Torque Control for IM using Fuzzy Logic. ACSE journal, Vol. 6, No. 2, June 2006, pp.19-26.
[7] K. Rajashekara: Propulsion System Issues in Electric and Hybrid Electric Vehicle Applications. IPEC-yokohama, 1995, pp. 93-98.
[8] C. C. Chan: Overview of Electric Vehicles-Clean and Energy Efficient Urban Transportation. The 7th International Conference on Power Electronics and Motion Control, Budapest, Hungary, 2-4 September 1996, V. 1, pp. K7-K15.
[9] K.T. Chau and Z. Wang: Overview of Power Electronic Drives for Electric Vehicles. HAIT Journal of Science and Engineering B, 2005, Vol 2, Issues 5-6, pp. 737-761.
[10] N. K. Mohanty, R. Muthu and M. S. Kumaran: A Survey on Controlled AC Electrical Drives. Medwell Journals, 2009, pp. 175-183.
[11] M. Zelechowski: Space Vector Modulated-Direct Torque Controlled (DTC–SVM) Inverter–Fed Induction Motor Drive. Ph.D. Thesis, Warsaw University of Technology, Warsaw–Poland, 2005.